COMMUNICATION

Dendritic maleimide functionalization of core–shell (γ-Fe₂O₃/polymer) nanoparticles for efficient bio-immobilization†

L. Mitcova,[ab] H. Rahma,[ab] T. Buffeteau,[ab] R. Clérac,[cd] L. Vellutini*[ab] and K. Heuzé*[ab]

A new route for the preparation of stable and water-dispersible core–shell γ-Fe₂O₃/polymer MNPs has been developed in order to ensure a selective and covalent immobilization of biomolecules using maleimide–thiol coupling chemistry. A high maleimide functionalization was achieved by the grafting of dendritic coupling agent *via* a convergent approach.

The integration of chemistry and nanotechnology in the field of molecular biology has resulted in a new emerging research area, which offers exciting opportunities for discovering new materials, processes, and phenomena.[1–4] In the last two decades, tremendous progress has been made in the development of magnetic particles on both synthetic and technological aspects.[2–7] Due to the simplicity in their use and their large surface-to-volume ratio, magnetic particles are nowadays the most common solid platform for immobilization and detection of biomolecules.[8–12] Among the major advances, important efforts have been dedicated to the development of highly functionalized magnetic nanoparticles (MNPs) for the immobilization of biomolecules.[8,9]

ªUniv. Bordeaux, ISM UMR 5255, F-33400 Talence, France. E-mail: karine.heuze@u-bordeaux.fr

ᵇCNRS, ISM UMR 5255, F-33400 Talence, France
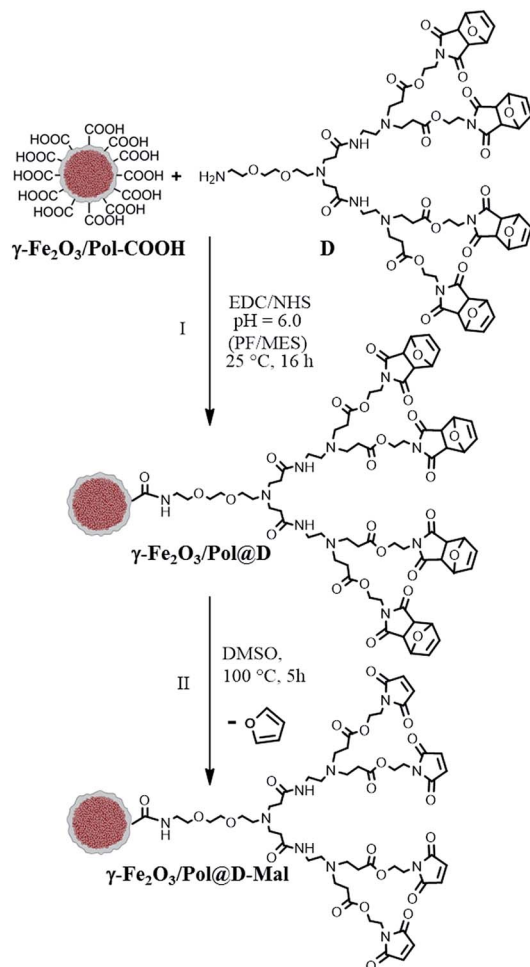
ᶜCNRS, CRPP, UPR 8641, F-33600 Pessac, France

ᵈUniv. Bordeaux, CRPP, UPR 8641, F-33600 Pessac, France

† Electronic supplementary information (ESI) available: Full experimental details for the synthesis of dendron **D**. ¹H NMR, ¹³C NMR, MS-ESI, FT-IR ATR spectra of organic compounds. Grafting and deprotection procedures. Immobilization tests procedures. γ-Fe₂O₃/**Pol@D** and γ-Fe₂O₃/**Pol@D-Mal** FT-IR ATR spectra. TEM image of native γ-Fe₂O₃/**Pol-COOH** MNPs. Zeta potential *vs.* pH measurements for γ-Fe₂O₃/**Pol@D-Mal** and γ-Fe₂O₃/**Pol-COOH** MNPs. Field dependence of magnetization at different temperatures for γ-Fe₂O₃/**Pol-COOH** and γ-Fe₂O₃/**Pol@D-Mal**. Temperature dependence of the magnetization saturation and of the coercive field for γ-Fe₂O₃/**Pol-COOH** and γ-Fe₂O₃/**Pol@D-Mal**. UV-Vis absorption spectra of **Au-SA** NPs solutions recovered after immobilization of the **Au-SA** NPs onto γ-Fe₂O₃/**Pol@D-Mal@Biot**. TEM image of γ-Fe₂O₃/**Pol@D-Mal** MNPs recovered after their incubation with **H₂N-PEG-Au NPs**. See DOI: 10.1039/c5ra17928a

In this context, one of the major focuses is to design MNPs, which would covalently bind biomolecules without disrupting their biological activity, and concomitantly limit nonspecific adsorption. Nevertheless it is obvious that the amount of covalently immobilized biomolecules is limited by the number of available functional groups at the MNP surface. Therefore, in this work we aimed to ensure a high number of functional groups at the MNP surface by its functionalization with dendritic coupling agent. The efficiency of this approach was demonstrated in our previous results, which showed an increase of the surface functionalization[13–15] together with a dendritic effect on the intrinsic physico-chemical properties of the materials.[16] In this study, the maleimide functional group was chosen for its biocompatibility and for its high selectivity towards thiol group of cysteine residue, naturally present or artificially introduced in biomolecules.[17–20] In this context, maleimide functionalization of nanoparticles surfaces is one of the well-studied strategies for bioconjugation of nanoparticles.[21–23] Taking into account that the number of cysteine residues naturally present in biomolecules is very scarce (in comparison with other functionalities as amino or carboxyl groups), the maleimide–thiol coupling chemistry enables a degree of control over biomolecular orientation and at the same time requires no additional reagent and generates no by-products (comparing to the EDC bioconjugate chemistry, for example). The Michael addition of thiol containing biomolecules to maleimide group is typically performed under mild conditions (in aqueous solutions or protic solvent at neutral pH and temperatures from 25 up to 37 °C), resulting in the formation of a stable thioether linkage.[20]

The functionalization of MNPs with dendritic structures can be achieved either by a divergent approach for which the dendritic structure is built step by step on MNPs' surface, or by a convergent strategy, according to which the dendritic structure is synthesized in a first step, and grafted onto the MNP surface in a second step.[24–26] In this work, the functionalization of MNPs with maleimide dendritic structure was achieved *via* convergent approach to ensure the preparation of dendritic

structures of high generation in large quantities and with no structural defects. To the best of our knowledge, the synthesis and the grafting of a maleimide dendritic structure linker is investigated for the first time at the surface of magnetic nanoparticles, while surface maleimide functionalization is generally achieved *via* commercial heterobifunctional linkers.

γ-Fe$_2$O$_3$ core–shell MNPs, γ-Fe$_2$O$_3$/Pol-COOH (Scheme 1) were used for the grafting of the maleimide functionalized dendritic coupling agent. These MNPs‡ are bearing carboxylic acid functionality in a high density, available for covalent functionalization. Dendron **D** (Scheme 1), containing an amine group as anchoring site and four maleimide functional groups (under furan protection form), was synthesized by a method used for Tomalia-type poly(amidoamine) (PAMAM) dendrimers (Scheme S1†).[27,28] Its inner backbone is composed of tri(ethylene glycol) chains as well as a poly(amidoamine) (PAMAM) dendritic part that confers a high colloidal stability in aqueous medium to the functionalized MNPs. In addition, the ethylene glycol chain is considered to be one of the most efficient chemical groups that limit the non-specific adsorption of proteins.[29–31]

The grafting of the dendron **D** on γ-Fe$_2$O$_3$/Pol-COOH MNPs proceeded *via* EDC/NHS chemistry (Scheme 1, step I). Then, the maleimide deprotection[32] (cleavage of furan) was achieved *via* retro Diels–Alder reaction by heating the particles up to 100 °C for 5 hours (Scheme 1, step II), generating maleimide functionalized MNPs (γ-Fe$_2$O$_3$/Pol@D-Mal).

The surface modification chemistry has been monitored *via* Fourier Transformed Infrared Spectrometry (FT-IR) using Attenuated Total Reflectance (ATR) mode. The subtraction of the native γ-Fe$_2$O$_3$/Pol-COOH MNPs' spectrum from the γ-Fe$_2$O$_3$/Pol@D MNPs' one (Fig. S1a†) clearly showed the presence of multiple absorption bands characteristic for the carbonyl groups of dendron **D** (Fig. S2†): in-phase C=O stretching band at 1775 cm^{-1}, out-of-phase C=O stretching band at 1703 cm^{-1}, C=O stretching band of ester groups at 1740 cm^{-1} and a broad shoulder around 1650 cm^{-1} that arises from the C=O amide 1 stretching mode. The substracted spectrum of γ-Fe$_2$O$_3$/Pol@D-Mal (Fig. S1b†) showed the disappearance of the furan ring deformation bands at 916, 878, 854 and 824 cm^{-1}, confirming the successful cleavage of furan protection. It can be also noted in Fig. S1a† the shift of the out-of-phase C=O stretching band from 1703 cm^{-1} to 1709 cm^{-1} after the maleimide deprotection. Finally, the intensity of the carbonyl bands points out the high content of available maleimide functional groups at the MNPs surface.

The integrity of the MNPs after grafting and deprotection (steps I and II, respectively) was observed by TEM (Fig. 1A and B, respectively). This result strongly supports that the surface chemistry does not affect the size and shape of the modified MNPs in comparison to the native γ-Fe$_2$O$_3$/Pol-COOH MNPs (Fig. S3†). The surface charge of the maleimide functionalized MNPs was estimated by zeta potential (ζ) measurements in aqueous solution and compared to the one of native particles (Fig. S4†). Upon functionalization, the isoelectric point shifts from 2.7 to 4.3 for native and maleimide functionalized MNPs
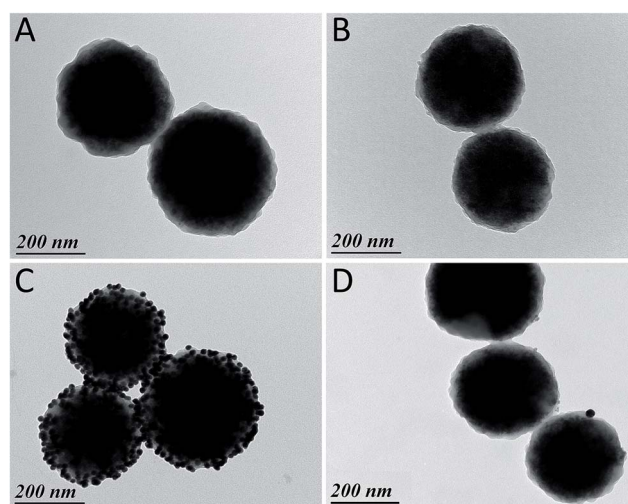

Scheme 1 Grafting of dendron D on γ-Fe$_2$O$_3$/Pol-COOH MNPs (step I) and maleimide group deprotection (step II).

Fig. 1 TEM image of: (A) MNPs obtained after the grafting of dendron D; (B) maleimide functionalized MNPs; (C) 15 nm SA-Au NPs immobilized on the surface of the biotin functionalized MNPs and (D) biotin functionalized MNPs recovered after their incubation with 20 nm H$_2$N-PEG-Au NPs.

(γ-Fe$_2$O$_3$/Pol@D-Mal), respectively. This effect is consistent with a maleimide surface modification that is less negatively charged than the original carboxylic acid MNPs.

These measurements revealed also that maleimide functionalized MNPs are stable in water medium at pH values higher than 5.0 and lower than 3.8 (when $|\zeta|$ values are >30 mV). It is likely that the dendritic shape of the functional linker plays a positive effect by preserving the stability of MNPs colloidal suspension in neutral water medium.[33]

The magnetic properties of the γ-Fe$_2$O$_3$/Pol@D-Mal MNPs were studied between 2 and 300 K monitoring the field dependence of their magnetization (Fig. S5†). Maleimide functionalized and native nanoparticles display virtually identical superparamagnetic properties. Below 150 K, a hysteresis effect appears on the M vs. H data. The thermal variation of the coercive field (that reaches 230 Oe at 1.8 K) is also strictly identical, confirming that the magnetic core of the nanoparticles remains intact after functionalization. This result is of crucial importance since many applications of MNPs require the integrity of their magnetic properties even after chemical surface modification.

Finally, the efficiency of maleimide functionalized MNPs (γ-Fe$_2$O$_3$/Pol@D-Mal) to react with thiol groups of biomolecules, was investigated according to the two steps strategy presented in Scheme 2. The first step consists in the coupling of γ-Fe$_2$O$_3$/Pol@D-Mal with commercially available thiol-modified biotin (HS-PEG-Biot) in neutral conditions to provide γ-Fe$_2$O$_3$/Pol@D-Mal@Biot MNPs. In a second step, commercially available 15 nm streptavidin coated gold NPs (SA-Au) were immobilized at the γ-Fe$_2$O$_3$/Pol@D-Mal@Biot surface via biotin–streptavidin affinity affording γ-Fe$_2$O$_3$/Pol@D-Mal@Biot@SA-Au. In that case, SA-Au NPs are used as nanoscale markers, which can be quantified by TEM and UV-Vis spectroscopy. Therefore, SA-Au NPs solutions were recovered after their use and analyzed by UV-Vis spectroscopy while γ-Fe$_2$O$_3$/Pol@D-Mal@Biot@SA-Au MNPs were examined by both UV-Vis spectroscopy and TEM (Fig. 1). TEM images of γ-Fe$_2$O$_3$/Pol@D-Mal@Biot@SA-Au (Fig. 1C) clearly showed a compact coverage of SA-Au NPs at the surface of MNPs. 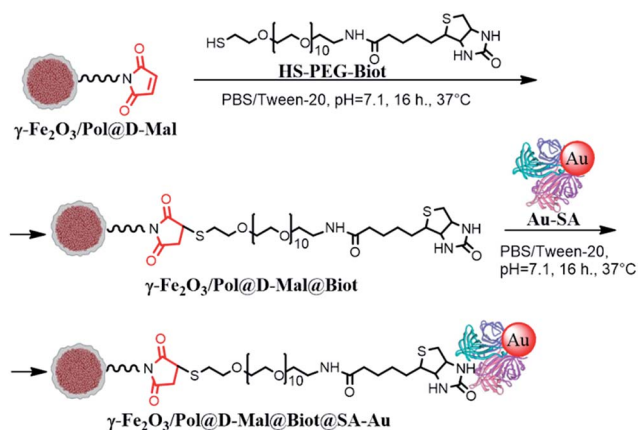Moreover, solution of MNPs became slightly pink after the addition of SA-Au NPs. It is worth mentioning that free SA-Au NPs were not observed in any samples, pointing out the efficiency of the washing procedure.

UV-Vis absorption spectra of the 15 nm SA-Au NPs solutions, recovered after the immobilization reactions, were recorded and a quantitative analysis was performed (Fig. S6†). According to the calibration curve performed on SA-Au NPs solutions, the high surface coverage of SA-Au NPs was confirmed. Indeed, 1.72×10^{12} SA-Au NPs (corresponding to 280 pmol of streptavidin) are immobilized per mg of γ-Fe$_2$O$_3$/Pol@D-Mal@Biot MNPs. Moreover, UV-Vis absorption spectrum of the γ-Fe$_2$O$_3$/Pol@D-Mal@Biot@SA-Au MNPs was recorded (Fig. 2). This spectrum undoubtedly confirmed the presence of the 15 nm SA-Au NPs on the surface of biotin functionalized MNPs. The shift of the plasmon absorption band from 526 to 545 nm was attributed to inter-particles coupling effects[34] resulting from the compact coverage of the gold nanoparticles.

These results indicated indirectly the remarkable high density of maleimide MNPs modification obtained comparing to other nanoparticles functionalization reported in the literature.[3,17–20,26] Also, it should be noted that no immobilization of 15 nm SA-Au NPs was observed in the case of their incubation with a solution of native γ-Fe$_2$O$_3$/Pol-COOH MNPs in same reaction conditions.

In parallel, the incubation of commercial 20 nm amino PEGylated gold nanoparticles (H$_2$N-PEG-Au NPs) with γ-Fe$_2$O$_3$/Pol@D-Mal@Biot was performed according to the same protocol to control the specificity of biotin–streptavidin affinity. As expected, the TEM study (Fig. 1D) confirmed that biotin functionalized MNPs (γ-Fe$_2$O$_3$/Pol@D-Mal@Biot) did not immobilize H$_2$N-PEG-Au NPs via non-specific adsorption.

Finally, the specificity of the thiol groups towards maleimide functionalized MNPs was investigated through the immobilization of H$_2$N-PEG-Au NPs on γ-Fe$_2$O$_3$/Pol@D-Mal following the same protocol used for the immobilization of HS-PEG-Biot. Indeed, even if maleimide reacts preferentially with thiol in

Scheme 2 Covalent coupling of thiol modified biotin with γ-Fe$_2$O$_3$/Pol@D-Mal followed by the immobilization of 15 nm SA-Au NPs via biotin–streptavidin affinity.
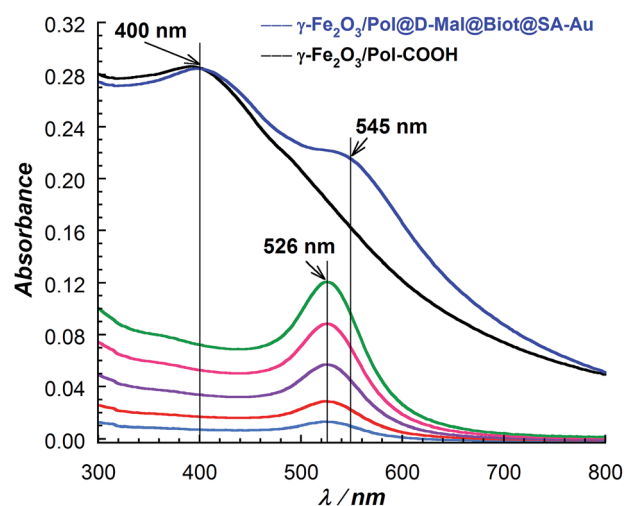

Fig. 2 UV-Vis absorption spectra of the solutions of native MNPs (solid line in black); γ-Fe$_2$O$_3$/Pol@D@Biot@SA-Au MNPs (solid line in dark blue) and SA-Au NPs solutions of different concentrations (solid lines in: light blue, red, violet, pink and green).

neutral pH conditions, primary amine may react to a lesser extend.[6] TEM analysis (Fig. S7†) revealed a poor number of H_2N-PEG-Au NPs immobilized at the surface of γ-**Fe₂O₃**/**Pol@D-Mal**.

Conclusions

In summary, we have developed highly maleimide functionalized MNPs (γ-**Fe₂O₃**/**Pol@D-Mal**), which are stable, resistant to non-specific adsorption, water dispersible, and efficient for specific and selective covalent immobilization of thiol containing biomolecules. As the engineering of functional surfaces remains one of the keys for optimizing immobilization of biomolecules, this work opens a broad range of potential uses especially because the maleimide functional group is of high interest in biomedicine for targeting, imaging, detection, diagnostic and therapeutic applications. In addition, our synthetic strategy can be readily extended to other functional groups efficient for bioconjugation applications and more generally for bionanotechnology.

Acknowledgements

Notes and references

‡ γ-Fe_2O_3 core–shell MNPs (300 nm, SD < 20%, carboxyl-adembeads) were purchased at Ademtech, France. These MNPs are coated with a polymer (cross-linked PS) shell bearing carboxylic acid functionality in a high density (COOH density: >350 μmol g^{-1}).

1 R. J. Koopmans and A. Aggeli, *Curr. Opin. Microbiol.*, 2010, **12**, 327.
2 M. de, P. S. Gosh and V. M. Rotello, *Adv. Mater.*, 2008, **20**, 4225.
3 W. R. Algar, D. E. Prasuhn, M. H. Stewart, T. L. Jennings, J. B. Blanco-Canosa, P. E. Dawson and I. L. Medintz, *Bioconjugate Chem.*, 2011, **22**, 825.
4 E. C. Wang and A. Z. Wang, *Integr. Biol.*, 2014, **6**, 9.
5 S. Singamanemi, V. N. Bliznyuk, C. Binek and E. Y. Tsymbal, *J. Mater. Chem.*, 2011, **21**, 16819.
6 A. H. Lantham and M. E. Williams, *Acc. Chem. Res.*, 2008, **41**, 411.
7 S. Laurent, D. Forge, M. Port, A. Roch, C. Robic, L. Vander Elst and R. N. Muller, *Chem. Rev.*, 2008, **108**, 2064.
8 K. E. Sapsford, W. R. Algar, L. Berti, K. B. Gemmill, B. J. Casey, E. Oh, M. H. Stewart and I. L. Medintz, *Chem. Rev.*, 2013, **113**, 1904.
9 L. H. Reddy, J. L. Arias, J. Nicolas and P. Couvreur, *Chem. Rev.*, 2012, **112**, 5818.
10 M. Colombo, S. Carregal-Romero, M. F. Casula, L. Gutierrez, M. P. Morales, I. B. Bohm, J. T. Heverhagen, D. Prosperi and W. J. Parak, *Chem. Soc. Rev.*, 2012, **41**, 4306.
11 Y. Li, X. Zhang and C. Deng, *Chem. Soc. Rev.*, 2013, **42**, 8517.
12 R. Chaudhuri and S. Paria, *Chem. Rev.*, 2012, **112**, 2373.
13 K. Heuzé, D. Rosario-Amorin, S. Nlate, M. Gaboyard, A. Bouter and R. Clérac, *New J. Chem.*, 2008, **32**, 383.
14 D. Rosario-Amorin, M. Gaboyard, R. Clérac, S. Nlate and K. Heuzé, *Dalton Trans.*, 2011, **40**, 44.
15 D. Rosario-Amorin, M. Gaboyard, R. Clérac, L. Vellutini, S. Nlate and K. Heuzé, *Chem.–Eur. J.*, 2012, **18**, 3305.
16 D. A. Tomalia, *New J. Chem.*, 2012, **36**, 264.
17 L. S. Wong, F. Khan and J. Micklefield, *Chem. Rev.*, 2009, **109**, 4025.
18 M. A. Stenzel, *ACS Macro Lett.*, 2013, **2**, 14.
19 P. M. S. D. Cal, G. J. L. Bernardes and P. M. P. Gois, *Angew. Chem., Int. Ed.*, 2014, **53**, 10585.
20 G. T. Hermanson, *Bioconjugate Techniques*, Academic Press, San Diego, 2nd edn, 2008.
21 D. Li, W. Y. Teoh, J. J. Gooding, C. Selomulya and R. Amal, *Adv. Funct. Mater.*, 2010, **20**, 1767.
22 T. Nguyen and M. B. Francis, *Org. Lett.*, 2003, **5**, 3245.
23 M. Mazur, A. Barras, V. Kuncser, A. Galatanu, V. Zaitzev, K. V. Turcheniuk, P. Woisel, J. Lyskawa, W. Laure, A. Siriwardena, R. Boukherroub and S. Szunerits, *Nanoscale*, 2013, **5**, 2692.
24 Y.-S. Shon and D. Choi, *Curr. Nanosci.*, 2007, **3**, 245.
25 D. A. Tomalia and J. M. Fréchet, *J. Polym. Sci., Part A-1: Polym. Chem.*, 2002, **40**, 2719.
26 A. L. Martin, L. M. Bernas, B. K. Rutt, P. J. Foster and E. R. Gillies, *Bioconjugate Chem.*, 2008, **19**, 2375.
27 G. R. Newkome and C. Shreiner, *Chem. Rev.*, 2010, **110**, 6338.
28 H. Rahma, T. Buffeteau, C. Belin, M. Degueil, B. Bennetau, L. Vellutini and K. Heuzé, *ACS Appl. Mater. Interfaces*, 2013, **5**, 6843.
29 K. Nakanishi, T. Sakiyama, Y. Kumada, K. Imamura and H. Imanaka, *Curr. Proteomics*, 2008, **5**, 161.
30 E. Ostuni, R. G. Chapman, R. E. Holmlin, S. Takayama and G. M. Whitesides, *Langmuir*, 2001, **17**, 5605.
31 S. R. Benhabbour, H. Sheardown and A. Adronov, *Macromolecules*, 2008, **41**, 4817.
32 A. Sanyal, *Macromol. Chem. Phys.*, 2010, **211**, 1417.
33 V. Gubala, X. le Guevel, R. Nooney, D. E. Williams and B. MacCraith, *Talanta*, 2010, **81**, 1833.
34 S. K. Ghosh and T. Pal, *Chem. Rev.*, 2007, **107**, 4797; Y. He, Q. S. P. Liu, L. Kong and Z. F. Liu, *Spectrochim. Acta, Part A*, 2005, **61**, 2861.